

# Extent of the participation of lattice oxygen from $\gamma$ -MnO<sub>2</sub> in VOCs total oxidation: Influence of the VOCs nature

Caroline Cellier, Valérie Ruaux, Christophe Lahousse,  
Paul Grange<sup>✱</sup>, Eric M. Gaigneaux<sup>\*</sup>

*Unité de catalyse et chimie des matériaux divisés, Université catholique de Louvain, B-1348 Louvain-la-Neuve, Belgium*

Available online 23 June 2006

## Abstract

Investigation of the total oxidation of *n*-hexane and trimethylamine as well as extensive characterizations of the catalyst after tests have been coupled to identify the mechanism of oxidation involved over a very active  $\gamma$ -MnO<sub>2</sub> catalyst. This work shows that the extent of the catalyst reduction, which is a consequence of the Mars and van Krevelen redox mechanism, depends on the nature of the organic molecule. Indeed, the nature of the VOC dictates its conversion level through its ability to reduce the catalyst and accelerate the incorporation rate of gaseous oxygen. © 2006 Elsevier B.V. All rights reserved.

**Keywords:** Manganese dioxide; Mars and van Krevelen mechanism; Nitrogen-containing volatile organic compound

## 1. Introduction

The catalytic oxidation of volatile organic compounds (VOCs) is widely applied in cleaning polluted effluents. Attention has also been focused on removal of unpleasant odor compounds [1–3] particularly nitrogen-containing compounds (N-VOCs). However, few authors [4,5] have compared the catalytic oxidation of N-VOCs to other classes of VOCs. In a previous work, we have investigated the total oxidation of *n*-hexane and trimethylamine over several oxide and noble metal catalysts [6]. This work showed that  $\gamma$ -MnO<sub>2</sub> was the most active catalyst to oxidize both molecules selectively into CO<sub>2</sub>, H<sub>2</sub>O and N<sub>2</sub>. The polyvalent character of  $\gamma$ -MnO<sub>2</sub> to convert efficiently both molecules makes it a very promising candidate to remove such compounds. In a recent contribution, we have moreover demonstrated that the activity of  $\gamma$ -MnO<sub>2</sub> catalyst is intrinsically linked to its surface area [7]. High surface area  $\gamma$ -MnO<sub>2</sub> catalyst represents thus a good candidate for real system applications. Although there have been some explanations about the changes encountered by this catalyst during the total

oxidation of *n*-hexane and ethylacetate [8], the mechanism of oxidation of  $\gamma$ -MnO<sub>2</sub> is still unclear.

Some fundamental works aiming at understanding the behavior of other manganese oxides (Mn<sub>2</sub>O<sub>3</sub>, Mn<sub>3</sub>O<sub>4</sub> and  $\beta$ -MnO<sub>2</sub>) can be found. Lahousse et al. [9] evaluated the activity of different manganese dioxide phases in relation to their crystallographic features and attributed the higher activity of  $\gamma$ -MnO<sub>2</sub> to its improved electronic and protonic conductivity. Busca and co-workers [10,11] oriented their studies towards the understanding of the formation of surface intermediates and of the reaction pathway mechanisms. Based on their infrared results, they suggested that a Mars and van Krevelen mechanism implying lattice oxygen occurs on Mn<sub>3</sub>O<sub>4</sub>. The kinetic study performed by Gandia et al. [12] showed that the acetone oxidation over Mn<sub>2</sub>O<sub>3</sub> follows a first-order with respect to the organic compounds and is independent of the oxygen concentration. An overall mechanism of the oxidation of VOCs on manganese oxides does not exist and thus a mechanism for  $\gamma$ -MnO<sub>2</sub> cannot be proposed. Moreover, the influence of a nitrogen atom present in the molecule to oxidize over MnO<sub>x</sub> systems has not yet been investigated in literature.

The aim of this study was thus to provide a better understanding of the VOC oxidation mechanism over  $\gamma$ -MnO<sub>2</sub> and to evaluate the impact of abating nitrogen-containing VOCs (N-VOCs) on its activity. For the comparison, *n*-hexane (Hex) was chosen as a representative hydro-carbonated VOC, while

<sup>\*</sup> Corresponding author. Tel.: +32 10 47 36 65; fax: +32 10 47 36 49.

E-mail address: [gaigneaux@cata.ucl.ac.be](mailto:gaigneaux@cata.ucl.ac.be) (E.M. Gaigneaux).

<sup>✱</sup> Deceased in July 2003.

trimethylamine (Tma) was selected as a representative N-VOC. A  $\gamma$ -MnO<sub>2</sub> sample of high surface area ( $\sim 100 \text{ m}^2/\text{g}$ ) was chosen to perform this work since it is a very good candidate for VOCs treatment systems. The objectives were indeed with this catalyst selection to approach operating conditions closed to real ones in terms of temperature, concentrations and space velocity. The modifications undergone by the  $\gamma$ -MnO<sub>2</sub> catalyst after different reaction conditions are characterized by XRD, XPS and potentiometric analyses.

## 2. Experimental

### 2.1. Catalyst

High surface area  $\gamma$ -MnO<sub>2</sub> sample ( $103 \text{ m}^2/\text{g}$ ) was provided by Erachem-Comilog Europe (Tertre, Belgium).

### 2.2. Characterization techniques

X-ray diffraction analyses were performed on a Siemens D5000 diffractometer using K $\alpha$  radiation of Cu ( $\lambda = 1.5418 \text{ \AA}$ ) and monocrystal sample holders. The  $2\theta$  range between  $2^\circ$  and  $85^\circ$  was scanned at a rate of  $0.02^\circ/\text{s}$ . Moreover, detailed scans of the  $2\theta$  range between  $35^\circ$  and  $40^\circ$  were performed with a step size of  $0.001^\circ/\text{s}$ .

N<sub>2</sub> physisorption measurements were performed on a Micromeritics ASAP 2010 instrument in the  $10^{-6} < p/p_0 < 0.99$  partial pressure range at  $-196^\circ\text{C}$ . The samples were degassed at  $150^\circ\text{C}$  under vacuum. Surface areas were computed using BET equation.

XPS analyses of Mn 2p, Mn 3s, N 1s, O 1s and C 1s were performed with a SSI X-Probe (SSX-100/206) photoelectron spectrometer from Surface Science Instrument (Fisons) equipped with a microfocused Al K $\alpha$  monochromatic X-ray source (1486.6 eV). Charge neutralization, energy and quantification procedure were described elsewhere [7,13].

Potentiometric titrations of the manganese valence state were achieved by titration of Mn<sup>IV</sup> species and total manganese ions in the samples. These analyses were performed at Erachem-Comilog Europe (Tertre, Belgium) (experimental details can be found in Ref. [13]).

DRIFTS spectra were collected with an IFS 55 Equinox spectrometer (Brüker) equipped with an air-cooled MIR source with KBr optics and a MCT detector. The powdered sample was placed inside an environmental temperature-programmed chamber (Spectra-Tech 0030-103). All spectra (200 scans with a resolution of  $4 \text{ cm}^{-1}$ ) were recorded in dehydrated helium.

### 2.3. Catalytic tests

Total oxidations of *n*-hexane or trimethylamine were carried out at atmospheric pressure in a conventional fixed bed reactor in the temperature range  $100\text{--}220^\circ\text{C}$  at a WHSV of  $72,000 \text{ h}^{-1}$ . The standard feed was composed of 125 ppm of *n*-hexane (Hex) and/or 250 ppm of trimethylamine (Tma) and 20 vol.% O<sub>2</sub> in N<sub>2</sub>. Mass transfer limitations and homogeneous reactions were checked not to occur with the reactor and conditions used.

The catalysts were heated in situ at the reaction temperature under a pure oxygen flow (50 ml/min). Before measuring the conversion, the temperature was maintained during 30 min. The activity was first measured at  $150^\circ\text{C}$  and the temperature was maintained during 23 h in order to stabilize the catalyst activity [7]. After this stabilization period, the temperature was then decreased to  $100^\circ\text{C}$  and subsequently increased by steps of 10 or 20 up to  $220^\circ\text{C}$ . At each temperature plate, temperature was maintained for 1 h in order to perform several analyses of the outlet.

## 3. Results

### 3.1. Activities

The light-off curves measured over  $\gamma$ -MnO<sub>2</sub> for the total oxidation of *n*-hexane and trimethylamine when introduced alone or in mixture are presented in Fig. 1. This figure shows that it is easier to oxidize 250 ppm of Tma than 125 ppm of Hex over the  $\gamma$ -MnO<sub>2</sub> catalyst. Moreover, these results also clearly demonstrate that the conversion of Tma is not significantly modified by the presence of Hex. In contrast, the conversion of *n*-hexane appears strongly inhibited by the presence of the amine. Indeed, the *n*-hexane conversion begins only above  $180^\circ\text{C}$ , i.e. when total conversion of trimethylamine is reached.

### 3.2. Characterizations

#### 3.2.1. Texture

N<sub>2</sub> physisorption measurements were performed over  $\gamma$ -MnO<sub>2</sub> samples before and after reactions. The results show that the variations of specific surface area, porous volume and pore diameter were negligible (see Table 1).

#### 3.2.2. Structure and oxidation state

XRD diffractograms of the catalysts show large and low intense lines characteristic of the nsutite ( $\gamma$ ) phase of MnO<sub>2</sub>. No phase appearance or disappearance was detected on the X-ray diffraction of the samples recovered after reactions. Only small band shifts were observed in some cases. These shifts can be used to characterize the modification of the bulk oxidation state

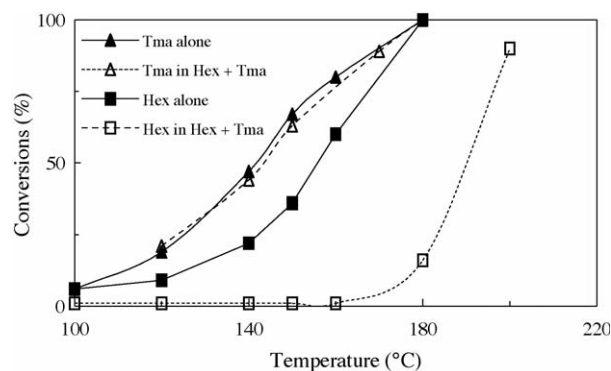


Fig. 1. Conversions of 125 ppm Hex (square symbols) and 250 ppm Tma (triangle symbols) alone (full symbols) or in mixture (open symbols) over  $\gamma$ -MnO<sub>2</sub> as a function of temperature.

Table 1

Characterizations of  $\gamma$ -MnO<sub>2</sub> by N<sub>2</sub> physisorption, XPS, XRD and potentiometric titration before and after catalytic reactions

Description of test conditions	Surface area (m <sup>2</sup> /g)	XPS		XRD $d_{hkl}$ (Å)	Potentiometric Mn AOS <sup>a</sup>
		Mn 3s-satellite (eV)	N/Mn ratio		
No test	103	4.9	0.00	2.41	3.9
Hex, 125 ppm, 150 °C for 23 h	n.m.	5.1	n.m.	2.41	3.8
Hex, 125 ppm, 200 °C <sup>b</sup>	102	4.9	n.m.	2.41	3.9
Hex, 125 ppm, 150 °C for 23 h + 1 h O <sub>2</sub>	n.m.	4.8	n.m.	2.41	n.m.
Hex, 125 ppm, 150 °C for 23 h + 1 h N <sub>2</sub>	n.m.	5.0	n.m.	2.42	n.m.
Tma, 250 ppm, 150 °C for 3 h	n.m.	5.1	0.06	2.44	n.m.
Tma, 250 ppm, 150 °C for 23 h	n.m.	5.1	0.21	2.44	3.5
Tma, 250 ppm, 200 °C <sup>b</sup>	100	5.0	0.09	2.43	3.8
Tma, 250 ppm, 150 °C for 23 h + 1 h O <sub>2</sub>	n.m.	5.1	0.16	2.44	n.m.
Tma, 250 ppm, 150 °C for 23 h + 7 h O <sub>2</sub>	n.m.	5.0	0.06	2.42	n.m.
Tma, 250 ppm, 150 °C for 23 h + 1 h N <sub>2</sub>	n.m.	5.2	0.20	2.45	3.4

n.m., not measured.

<sup>a</sup> AOS, average oxidation state.<sup>b</sup> Test stopped at 100% conversion to carbon monoxide and water.

of  $\gamma$ -MnO<sub>2</sub> [13,14]. Reduction of the catalyst bulk was evaluated through the measurement of the position of  $\gamma$ -MnO<sub>2</sub> main line positioned at  $2\theta = 37.2^\circ$  ( $d = 2.41$  Å) in the sample before test. Indeed, a reduction of the bulk of  $\gamma$ -MnO<sub>2</sub> causes a shift of its main XRD lines towards higher  $d$  (lower  $2\theta$ ) values [13,14]. Besides XRD measurements, the reduction of the catalyst bulk on some samples was also checked using a potentiometric titration method. The average oxidation state of manganese in  $\gamma$ -MnO<sub>2</sub> is equal to 3.9 before test.

The surface oxidation state of Mn can be accurately evaluated by means of the difference of binding energy between the Mn 3s peak and its satellite. A reduction of the manganese induces an increase of this distance [13,15]. A  $\pm 0.1$  eV error on the Mn 3s splitting must be taken into account.

Table 1 gives the results of the characterizations of  $\gamma$ -MnO<sub>2</sub> before and after reactions by XPS, XRD and potentiometric titration. After reaction with both molecules at 150 °C, XPS measurements indicated that a slight reduction of the catalyst surface occurred, as shown by the increase of the Mn 3s band split distance. A deep reduction of the bulk was also noticed when the reaction was performed with trimethylamine ( $d$  shift from 2.41 to 2.44 Å and the average oxidation state (AOS) of Mn decrease from 3.9 to 3.5). However, such a strong bulk reduction was not observed when the test was performed with *n*-hexane. At 200 °C, i.e. when total oxidations of both molecules were reached, surface reoxidation (decrease of the Mn 3s splitting) as well as the bulk one were observed with both molecules.

Additional characterizations of the catalyst were performed after reaction with trimethylamine or *n*-hexane at 150 °C then flushing the catalyst under pure O<sub>2</sub> or N<sub>2</sub> flows at 150 °C. Table 1 shows that these experiments change the oxidation state of the catalyst in different ways. The following effects were indeed observed:

- After reaction with *n*-hexane: 1 h of flushing under an oxygen flow induces a reoxidation of the catalyst surface while 1 h of nitrogen flushing leads to a slight reduction of the catalyst.

- After reaction with trimethylamine: 1 h of flushing under the oxygen flow does not change the oxidation state of the catalyst. But, after an increased time of flowing to 7 h, the catalyst surface and more significantly the catalyst bulk appeared markedly reoxidized compared to the catalyst recovered just after the reaction. In contrast, a flushing under the nitrogen flow causes a reduction of the surface and bulk of the catalyst.

### 3.2.3. Surface species

In addition to the evaluation of the surface oxidation state, XPS also allows to evaluate deposition or modification of surface species at the surface. Since sample surfaces are always contaminated with carbon species, a quantitative analysis of carbon that would have been deposited during reactions was not relevant. In contrast, nitrogen species were significantly detected at the catalyst surface after reaction with trimethylamine. All samples that had been in contact with the amine present a broad peak in the 398–401 eV region. This peak position is consistent with nitrogen present in organic compounds or NH<sub>x</sub> species [16]. Whatever the reaction conditions, no change of N 1s and C 1s peak shape was observed.

The N/Mn ratios were measured and used to evaluate the surface nitrogen content on the samples after reaction with trimethylamine (see Table 1). As seen in Table 1, the N/Mn ratio increases with the reaction time at 150 °C to reach the value of 0.21, then decreases when complete conversion is obtained at 200 °C. The N/Mn ratio was hardly not modified by the nitrogen flushing. However, a decrease of the nitrogen content was induced by oxygen flushing at 150 °C. Moreover, the higher the flowing time was, the lower the measured N/Mn ratio was.

### 3.3. DRIFTS study of the adsorption/desorption of trimethylamine

The adsorption experiment was conducted as followed: the sample was first pretreated under oxygen at 150 °C then cooled

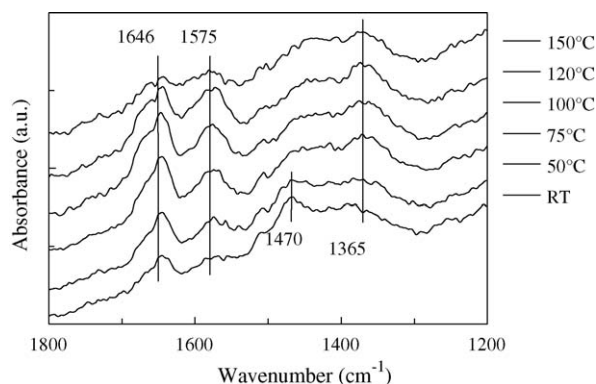


Fig. 2. DRIFTS spectra recorded when heating the catalyst from room temperature to 175 °C under an inert and dehydrated helium flow after adsorption of trimethylamine over  $\gamma$ -MnO<sub>2</sub>.

down to room temperature. The analysis cell was then flushed under a pure dehydrated flow of helium followed by the adsorption under a flow of diluted trimethylamine (0.5 vol.% in N<sub>2</sub>) during 0.5 h, and an additional purge with pure helium. This experiment shows that trimethylamine is adsorbed on  $\gamma$ -MnO<sub>2</sub> at room temperature. But, the flushing under inert helium for 1 h following the adsorption induces a decrease of the intensity of the bands at 1470, 2840 and 2781 cm<sup>-1</sup>, corresponding to C–H vibration bands in the methyl groups of trimethylamine, and the appearance of a band at 1646 cm<sup>-1</sup>. This band at 1646 cm<sup>-1</sup> could be assigned to *N,N*-dimethylformamide as previously reported by Guglielminotti and Boccuzzi [17] in their study of the oxidation of TMA and as also supported by the fact that this molecule was detected as a reaction intermediate during catalytic tests.

The “desorption” experiment was then conducted by heating the sample under a pure dehydrated helium flow. Spectra were recorded at 50, 75, 100, 120, 130, 140, 150 and 175 °C, each one after 30 min of temperature stabilization. As shown in Fig. 2, heating the catalyst under inert helium leads to the complete disappearance of the C–H vibrations bands, increase of the band at 1646 cm<sup>-1</sup> and appearance of bands at 1365 and 1575 cm<sup>-1</sup>. The two last bands could be assigned to carbonates species [17]. This experiment clearly demonstrates that an oxidation of the amine takes place in absence of any gaseous oxygen.

### 3.4. Kinetic study

First, to check that no mass transfer affect the kinetics, tests were performed at constant space velocity but varying the amount of catalyst (0.05, 0.1 and 0.2 g) and correspondingly the flow rates (50, 100 and 200 ml min<sup>-1</sup>) introduced in the reactor. Then additional tests were performed with 0.1 g of catalyst but varying the particle sizes (100–200, 200–315 or 315–500  $\mu$ m). All these tests showed the steadiness of the *n*-hexane and trimethylamine conversions establishing that neither external nor internal mass transfer limitations occur.

The kinetic study was then performed by varying independently the oxygen or the *n*-hexane concentrations and keeping the other reactant concentration and the total flow constant [18]. The redox model proposed by Mars and van

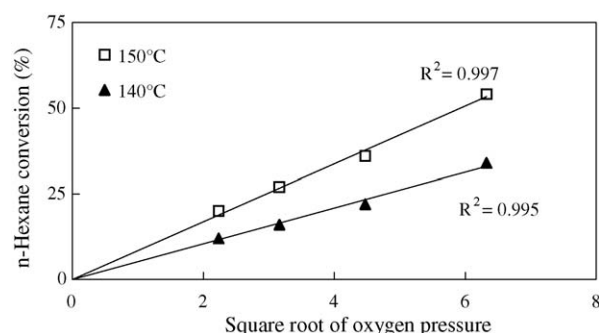


Fig. 3. *n*-Hexane conversion over  $\gamma$ -MnO<sub>2</sub> as a function of the square root of the oxygen pressure.

Table 2

Comparison of Hex and Tma oxidation data on activity and kinetic parameters

Experimental data	Hex	Tma
$E_a$ (kJ/mol)	70	52
Reaction rate constant, $k_0$	0.016	0.033
Feed concentration (ppm)	125	250
Oxygen stoichiometric factor	9.5	5.25
Conversion (%)	36	57
Oxygen consumption (ppm)	~430	~750

Krevelen [19] has been widely used and validated to describe many oxidation reactions including total oxidation of VOCs [20,21]. The model expression developed by Mars and van Krevelen was combined with the model equation for an integral plug-flow reactor to give the following relation:

$$C = \frac{wk_0[\text{O}_2]_0}{\gamma F[\text{R}]_0}$$

where  $C$  is the experimental conversion,  $w$  the catalyst weight,  $k_0$  the reaction rate constant,  $[\text{O}_2]_0$  and  $[\text{R}]_0$  are the initial concentration of oxygen and reactant respectively,  $\gamma$  the stoichiometric coefficient for the total oxidation of the reactant and  $F$  is the reaction mixture flow rate.

This relation was used to check the reaction orders towards the oxygen and the reactant. A zero-order with respect to *n*-hexane in accordance with the chosen experimental model has been verified. Moreover, this study also showed that the reaction order for O<sub>2</sub> is close to 1/2. Fig. 3 illustrates this by the good correlations obtained between the square root of oxygen pressure and the corresponding experimental conversions.

The apparent activation energies ( $E_a$ ) were also determined for the oxidation of trimethylamine or *n*-hexane alone (Table 2) [18]. The values of the apparent activation energy are well in the range of the activation energies measured in literature for VOC oxidations [20].

## 4. Discussion

### 4.1. Overall mechanism

According to the Mars and van Krevelen mechanism [19], oxidation of adsorbed hydrocarbons proceeds through lattice



oxygen leaving reduced active sites, while regeneration of used sites occurs via reoxidation with the molecular oxygen of the gas feed. As demonstrated below, the characterizations after tests and the DRIFTS study support the occurrence of such mechanism.

Characterizations of the catalysts after reactions performed with trimethylamine or *n*-hexane at a temperature giving 50% of conversion, showed a reduction of the oxidation state of  $\gamma$ -MnO<sub>2</sub>. But, a reoxidation of the catalyst occurred at higher temperature. Thus, oxidation–reduction cycles of the manganese oxide take place during the reaction. The catalyst is partially reduced as long as the reduction rate of the catalysts (oxidation of the hydrocarbon) is superior to the reoxidation rate. With increasing temperature, reaction rate grows and the catalyst reoxidation rate becomes faster than the oxygen consumption (a reoxidation of the catalyst was observed at 220 °C). The reoxidation of the catalyst seems to be the most difficult step of the reaction at low temperature (150 °C).

Flushing the catalyst with a nitrogen flow after reaction at 150 °C induced a higher reduction of the catalyst (see Table 1) due to the conversion of some adsorbed species at the surface. Moreover, the DRIFTS study showed that the oxidation of adsorbed trimethylamine into more oxidized species (detection of *N,N*-dimethylformamide and carbonate species) occurs in an inert atmosphere. These results clearly demonstrate that oxidation of adsorbed organic compounds takes place in the absence of gas phase oxygen. Lattice oxygen from the catalyst can thus participate to the oxidation of the hydrocarbons.

No apparent modification of the overall mechanism over  $\gamma$ -MnO<sub>2</sub> is detected when N-VOC is considered.

In addition to characterization proofs, our kinetic study has shown that a zero-order with respect to Hex in accordance with the redox model developed by Mars and van Krevelen has been found. Moreover, the reaction order for O<sub>2</sub> is close to 1/2. These observations confirm that the oxidation of VOCs follows a Mars and van Krevelen mechanism limited by the catalyst reoxidation. Moreover, the reaction order of oxygen close to 1/2 suggests that the dissociation of the adsorbed molecular oxygen into atomic oxygen species is a reversible step that controls the nature of the rate-determining active centers.

#### 4.2. Influence of the molecule on the activity and reduction state of the catalyst

At 150 °C, the conversion and the associated consumption of oxygen are higher in the case of trimethylamine than with *n*-hexane (see Table 2). Moreover, the apparent activation energy found for the reaction with trimethylamine is inferior to that of *n*-hexane. As the mechanism of oxidation is a Mars and van Krevelen one where we evidenced that the reoxidation is the most difficult step, the apparent  $E_a$  should thus represent the energy required to reoxidize the active sites by oxygen. As  $E_{a,Tma}$  is inferior to  $E_{a,Hex}$ , less energy is required to reoxidize the active sites reduced by the amine. Moreover, characterizations of the catalysts recovered after reaction at 150 °C show that the trimethylamine induced a higher bulk reduction than *n*-hexane (see Table 1). These results clearly show that the nature

of the molecule has an influence on its conversion and on the catalyst reduction.

First, it could be suggested that lattice oxygen coming from the bulk are involved in a higher extent in the oxidation of the amine through the reoxidation of the active reduced sites. But, this assumption would imply that the catalyst is not at steady state and that it will continue to get more and more reduced as the reaction proceeds. This hypothesis must be discarded since characterizations of the catalyst recovered after 3 or 23 h of reaction at 150 °C show that the catalyst reduction is fast and stable (see Table 1).

It can be stated the adsorption strength of trimethylamine is stronger than that of *n*-hexane given that the conversion of this latter is completely inhibited by the presence of the amine (see Fig. 1). Due to its higher strength of adsorption, it is likely that the amine adsorbed and is converted on additional sites than *n*-hexane. Moreover, we can assume that the trimethylamine is a stronger reductant due to the higher polarizability of the molecule. The higher adsorption strength and/or the higher reducing power of the trimethylamine on the catalyst could explain the deeper reduction of the catalyst observed with the amine compared to hexane. Over a MoO<sub>3</sub> catalyst, Bertinchamps and Gaigneaux [22] have shown that slightly reduced oxides are more oxidant than fully oxidized ones since they can exchange oxygen more easily. Similarly, it is suggested that the higher extent of MnO<sub>2</sub> reduction induced by the amine engenders a faster diffusion of gaseous oxygen, adsorption and dissociation at the surface active sites. This faster incorporation of oxygen on the active sites is assumed to explain the higher conversion as well as the lower activation energy observed for the reaction with the amine.

## 5. Conclusions

The total oxidation of volatile organic compounds over  $\gamma$ -MnO<sub>2</sub> takes place through a Mars and van Krevelen mechanism. The kinetic study showed that the oxidation of *n*-hexane follows a half-order with respect to the oxygen and is independent of the VOC concentration. The presence of nitrogen into the molecule to oxidize does not change this overall mechanism.

The conversion is however influenced by the nature of the volatile organic compounds, which modifies the extent of catalyst reduction. The increase of the catalyst bulk reduction induces a higher rate of oxygen mobility and participation to the Mars and van Krevelen cycle.

## Acknowledgements

Dr. M.-F. Piton and Erachem-Comilog Europe (Tertre, Belgium) are gratefully acknowledged for providing the manganese dioxide and performing the manganese potentiometric titration measurements. This work was supported by the “Direction Générale des Technologies, de la Recherche et de l’Energie (DGTRE)” of the “Région Wallonne” (Belgium) (convention no 971/3667), the Fonds Spécial de la Recherche (FSR) of the Catholic University of Louvain, and the “Fonds

National de la Recherche Scientifique (FNRS)” of Belgium. The involvement of the laboratory in the Coordinated Action “CONCORDE” as work package leader; in the Network of Excellence “FAME” of the EU 6th FP, in the IUAP network: “Supramolecularity” sustained by the “Service public fédéral de programmation politique scientifique” (Belgium) are also acknowledged.

## References

- [1] Y. Ono, Y. Fujii, H. Wakita, K. Kimura, T. Inui, *Appl. Catal. B* 16 (1998) 227.
- [2] N. Watanabe, H. Yamashita, H. Miyadera, S. Tominaga, *Appl. Catal. B* 8 (1996) 405.
- [3] H. Kuwabara, T. Okuhara, M. Misono, *Chem. Lett.* 6 (1992) 947.
- [4] D. Pope, D.S. Walker, R.L. Moss, *Atmos. Environ.* 12 (1978) 1921–1927.
- [5] S.F. Tahir, C.A. Koh, *Chemosphere* 38 (9) (1999) 2109–2116.
- [6] C. Cellier, S. Lambert, V. Ruaux, C. Lahousse, P. Grange, J.-P. Pirard, B. Heinrichs, E.M. Gaigneaux, in: P. Forzatti, G. Groppi, P. Ciambelli, D. Sannino (Eds.), *Catalytic Combustion*, vol. 2, Polipress, Milano, 2005, p. 199.
- [7] C. Cellier, S. Lambert, E.M. Gaigneaux, C. Poleunis, V. Ruaux, P. Eloy, C. Lahousse, P. Bertrand, J.-P. Pirard, P. Grange, *Appl. Catal. B*, 2006, in press.
- [8] C. Lahousse, C. Cellier, B. Delmon, P. Grange, *Stud. Surf. Sci. Catal.* 130A (2000) 587.
- [9] C. Lahousse, A. Bernier, E. Gaigneaux, P. Ruiz, P. Grange, B. Delmon, *Stud. Surf. Sci. Catal.* 110 (1997) 777.
- [10] G. Busca, E. Finocchio, V. Lorenzelli, G. Ramis, M. Baldi, *Catal. Today* 49 (1999) 453.
- [11] M. Baldi, E. Finocchio, F. Milella, G. Busca, *Appl. Catal. B* 16 (1998) 43.
- [12] L.M. Gandia, A. Gil, S.A. Korili, *Appl. Catal. B* 33 (2001) 1–8.
- [13] C. Cellier, V. Vromman, V. Ruaux, P. Grange, E.M. Gaigneaux, *J. Phys. Chem.* 108 (2004) 9989.
- [14] W.C. Maskell, J.A.E. Shaw, F.L. Tye, *J. Appl. Electrochem.* 12 (1982) 101.
- [15] D.A. Shirley, *Phys. Scripta* 11 (1975) 117.
- [16] J.F. Moulder, W.F. Stickle, P.E. Sobol, K.D. Bomben, *Handbook of X-ray Photoelectron Spectroscopy*, Perkin–Elmer, USA, 1992.
- [17] E. Guglielminotti, F. Boccuzzi, *Mater. Chem. Phys.* 29 (1991) 387.
- [18] C. Cellier, PhD Thesis, Louvain-la-Neuve, 2003, p. 290.
- [19] P. Mars, D.W. van Krevelen, *Chem. Eng. Sci.* 3 (1954) 41 (Special Supplement).
- [20] S.K. Gangwal, M.E. Mullins, J.J. Spivey, P.R. Caffrey, B.A. Tichenor, *Appl. Catal.* 36 (1988) 231.
- [21] I.S. Jaswal, R.F. Mann, J.A. Juusola, J. Downie, *Can. J. Chem. Eng.* 47 (1969) 284.
- [22] F. Bertinchamps, E. Gaigneaux, *Catal. Today* 91–92 (2004) 105.